

7th Groundwater Symposium of the  
International Association for Hydro-Environment Engineering and Research (IAHR)

## Laboratory-scale investigation of two-phase relative permeability

L. Moghadasi<sup>a\*</sup>, A. Guadagnini<sup>b,c</sup>, F. Inzoli<sup>a</sup>, D. Colapietro<sup>a</sup>, M. Bartosek<sup>d</sup> and  
D. Renna<sup>d,†</sup>

<sup>a</sup> Politecnico di Milano, Department of Energy, via Lambruschini 4, 20156 Milan, Italy.

<sup>b</sup> Politecnico di Milano, Department of Civil and Environmental Engineering, piazza L. Da Vinci 32, 20133 Milan, Italy.

<sup>c</sup> University of Arizona, Department of Hydrology and Water Resources, Tucson, AZ 85721, USA.

<sup>d</sup> Eni Exploration & Production, Petroleum Engineering Laboratories, 20097 Milan, Italy.

---

### Abstract

We present experimental investigations of two-phase (oil and water) relative permeability of laboratory scale rock cores through a joint use of direct X-ray measurement and flow-through investigations. Experimental data embed key information relating relative permeability to observables. In this context, direct measurement of in-situ fluid saturation through X-Ray techniques has the unprecedented ability to characterize key processes occurring during the displacement of immiscible fluids through natural permeable materials. We illustrate the benefit of employing direct X-Ray measurements of fluid saturation through a set of laboratory experiments targeted to the estimate of two-phase relative permeabilities of homogeneous samples (sand pack and Berea sandstone core). Data are obtained for a range of diverse fractional flow rates and provide information at saturations ranging from irreducible water content to residual oil saturation. Our X-Ray saturation data are consistent with an interpretation of measured relative permeabilities as associated with water-wet rock conditions. The comparison of different preample samples result high displacement efficiency and recovery factor corresponds to the high permeable and well-connected pores.

© 2015 The Authors. Published by Elsevier B.V. This is an open access article under the CC BY-NC-ND license (<http://creativecommons.org/licenses/by-nc-nd/4.0/>).

Peer-review under responsibility of the Scientific Committee of the IAHR Groundwater Symposium 2014

*Keywords:* Porous Media; Two-phase Relative Permeability; X-ray Saturation Measurement; Laboratory Experiments.

---

\* Corresponding author. Tel.: +39 02 2399 8431.

E-mail address: [leili.moghadasi@polimi.it](mailto:leili.moghadasi@polimi.it)

## 1. Introduction

Two-phase flow through porous media is of critical relevance in geothermal, nuclear, and petroleum engineering applications. Estimates of relative permeabilities and their analysis by means of appropriate relative permeability models are at the core of the development and validation of reservoir simulation models [1]. Relative permeability is an important parameter in reservoir simulations as it conditions the estimate of the ultimate recovery from a reservoir. Permeability values depend largely on the proportions between volume fractions of fluids in a test sample [2]. The characterization of multi-phase flow in porous media is typically described by way of relative permeability curves. A variety of experimental techniques for assessing relative permeability curves are available [1, 3-6]. Three types of laboratory settings are considered to this end, i.e., (i) steady-state (SS), (ii) unsteady-state (US) or displacement, and (iii) centrifuge methods.

Comparison between results based on US and SS is presented in [7]. The authors perform a repeatability study and a sensitivity analysis of permeability estimates to parameters such as oil viscosity and imposed flow regime. Some examples of the application of the steady-state methods are found in [8, 9]. These include, e.g., the Penn-State method, the Hassler method, the Single-Sample Dynamic method, and the Hafford method. Unsteady-state techniques are the less time consuming methodologies which can be employed to estimate relative permeabilities [10, 11]. In these settings, saturation equilibrium is not attained and an entire set of curves representing the dependence of relative permeability on saturation can be obtained in a few hours [12, 13]. Some authors investigated the effect of flow rate, pressure, viscosity and temperature on measurements of water-oil relative permeability using SS settings. They found dependency of relative permeability on pressure, viscosity and temperature and observed a lack of dependence from flow rate [14, 15]. Avvram et al.[16] focused on pore-scale mechanisms and flow regimes of steady-state two-phase flow and their relation to relative permeabilities.

The precise evaluation of fluid saturations is critical to ensure appropriate estimates of relative permeability, relying on common interpretive models. Linear X-ray scanners are increasingly employed to yield real time measurements of fluid saturations in cores employed in laboratory tests [17]. Linear X-ray scanners are often used to characterize fluid saturations within core plugs during flow tests. The intensity of X-rays absorption is a function of materials making up the host rock. The reduction of intensity of an X-ray beam as it passes through a core plug depends on the residing fluids [18]. Behin et al. [19] describe interpretations of two-phase immiscible fluid flow with low viscosity ratio in water wet rocks by using X-ray in situ local saturation data.

Here, we perform a set of two-phase steady-state relative permeability measurements on a water-wet homogeneous confined sand pack and a Berea Sandstone core at ambient condition. We implement a joint use of traditional flow-through investigations and direct X-ray saturation monitoring to measure the saturations. The results are consistent with the water-wet nature of the rock system. A variety of injection flow rates are applied under both imbibition and drainage conditions.

## 2. Materials and methods

### 2.1. Porous media

A column of water-wet quartz sand-pack and a Berea sandstone core sample are considered in our experiments. Each of the samples is placed inside a rubber sleeve with an inner diameter of 3.81 cm. The sand-pack is constructed by packing of quartz sand (for a total length of 30 cm) and placing a layer (1 cm thickness) of coarse sand at the top and at the bottom of the column. Table 1 lists the characteristics of the samples.

Table 1. Main characteristics of the core samples.

|                                  | Sand-pack | Berea sandstone |
|----------------------------------|-----------|-----------------|
| Length [cm]                      | 30        | 30              |
| Diameter [cm]                    | 3.81      | 3.81            |
| Water absolute permeability [mD] | 2800      | 30              |
| Air permeability [mD]            | 3300      | 120             |
| Pore volume [ml]                 | 135       | 66              |
| Porosity [%]                     | 37        | 17              |

## 2.2. Fluids Characterization

The fluids used in the displacement experiments are brine and isoparaffinic mineral oil. The brine is tagged with X-ray absorbing chemicals (NaBr for the sand-pack and KBr for the Berea core sample) to allow for fluid saturation monitoring and to increase the contrast between oil and water X-ray absorption characteristics. Table 2 lists the properties of these fluids.

Table 2. Fluid properties.

|                      | Sand-pack | Berea sandstone |
|----------------------|-----------|-----------------|
| Oil viscosity [cp]   | 1.74      | 1.74            |
| Brine viscosity [cp] | 0.97      | 1.03            |

## 2.3. Experimental Setup

Figure 1 depicts a sketch of the experimental setup. It consists of Hassler-type core holders (TEMCO FCH-1.5m) containing water-wet samples, X-Ray saturation monitoring (Core Lab Instruments - Reservoir Optimization) and close loop pumping system. The experiments have been performed upon relying on the steady state method. All experiments are performed at 25°C. The X-ray apparatus which is employed to perform fluid saturation measurements includes generator and detector, composite carbon core holder and data acquisition device. An aluminium blocks are used as a calbrtaion before each scanning to compensate for X- ray fluctuation. The samples are positioned vertically inside a Hassler-type core holder and are subject to a confinement pressure of 30 bars. The samples are scanned from bottom to top of the samples of the system by applying an electric potential of 55 kV and a current of 30 mA. The core is scanned before, during (depending on the duration of the flow experiment) and after each flooding cycle. A phase separation burette closes the loop and permits direct volumetric readings. Reinjection of the oil and water from the separator to the core is then performed by dual piston volumetric pumps (Pharmacia LKB pump P-500). Two pressure transducers are employed to measure continuously the pressure drop across the core. Experiments are conducted in the presence of diverse fluid flow rates. Saturation equilibrium is attained for each flow rate.

## 2.4. Experimental procedure

SS experiments are sketched in Fig 2. A steady-state relative permeability experiment is performed by starting with complete saturation of the samples with brine (Step A). During this step, X-ray measurements are taken for calibration against the brine. A series of fluid displacements is then performed to saturate the samples with oil and perform the X-Ray calibration to oil (Step B). Irreducible

water saturation ( $S_{wi}$ ) is measured and oil permeability is assessed at these conditions. Joint injection of oil and water is then performed by applying a total constant flow rate of oil and water corresponding to 480 [ml/h] and 30 [ml/h] for sand-pack and Berea core sample, respectively. We conducted SS imbibition experiments by performing diverse joint-injections of oil and water with increasing the water) and decreasing the oil flow rates (Step C-E). We repeated the same procedure for SS drainage experiments while by increasing and decreasing the oil and brine flow rates, respectively. Note that each step takes more than one day to attain equilibrium. Residual oil saturation ( $S_{or}$ ) and Irreducible water saturation ( $S_{wi}$ ) are established at the end of the imbibition (Step F) and drainage (Step B) processes, respectively.

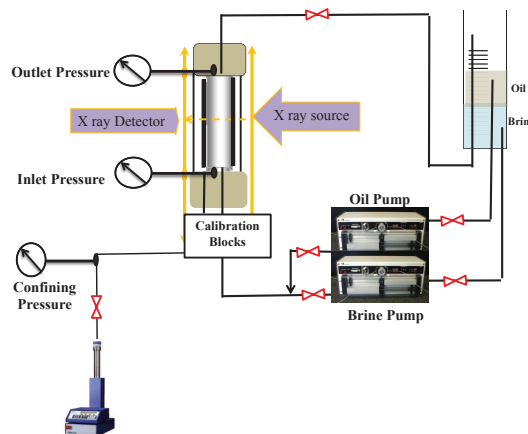


Fig. 1. Sketch of the experimental Setup.

The average fluid saturation and the pressure drop across the core are measured at equilibrium, when the saturation profiles and the pressure drop are stable. X-ray scans are performed after each step for the assessment of saturation profiles. Relative permeabilities are finally calculated upon applying Darcy's law and using average core saturation from X-ray in-situ measurements. The absolute permeability to water is determined through application of Darcy's law to the core under full saturation with brine ( $S_w = 1$ ). Then saturation is simply calculated by linear interpolation of brine and oil core scans. Error analysis is performed, resulting in an estimated accuracy of  $\pm 2\%$  for the in-situ saturation measurements. An irreducible water saturation of 19 % (Sand-pack) and 42% (Berea sandstone) are measured. The high  $S_{wi}$  in the Berea sample is due to low connectivity of pores which causes trapping of water during the invasion process. The low  $S_{wi}$  in the sand-pack reveals high displacement efficiency of water by oil.

### 3. Results and discussion

Figure 3 depicts the imbibition relative permeability curves versus average core saturation obtained from X-ray in-situ measurements for the tested core samples. A crossover of water and oil relative permeability is observed at 77% and 60% water saturation for the sand-pack and Berea core sample, respectively. Wettability of the rock can be determined as a function of the saturation corresponding to the crossing point between the relative permeability curves of water ( $K_{rw}$ ) and oil in the oil-water system ( $K_{row}$ ). The crossing points observed in our experiments ( $S_w \geq 50\%$ ) are consistent with an interpretation of the estimated relative permeabilities as being associated with water-wet rock conditions. Regarding water end relative permeabilities a good relationship is observed between water end relative

permeabilities and conductivity (Fig. 3). The well-connected pores (Sand-pack) have lower irreducible water saturation and larger water relative permeability. High irreducible water saturation and low relative permeability for Berea core sample with respect to sand-pack is due to the nature of the core sample. There might be significant capillarity effects and trapping of non-wetting phase while two phases are moving. The non-wetting phase is typically trapped in pores and will not allow the flow of wetting phase. Figure 4 depicts the average core saturation obtained from X-ray in-situ measurements and relative permeability values corresponding to imbibition and drainage processes. The results of drainage and imbibition relative permeabilities present dependency of water relative permeability on water saturation. It can be observed that hysteresis is larger for the oil than for the water relative permeability.

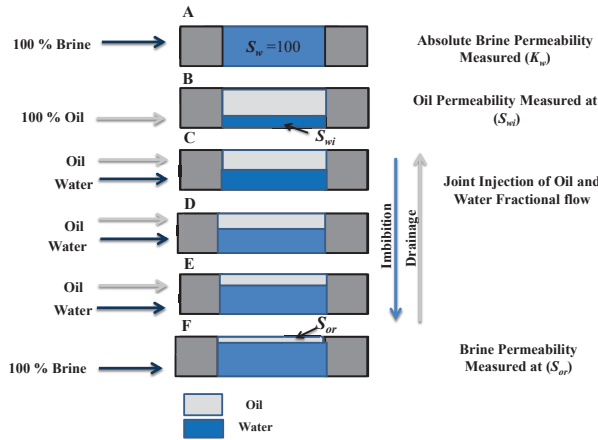


Fig. 2. Steady-State Imbibition and Drainage Procedures.

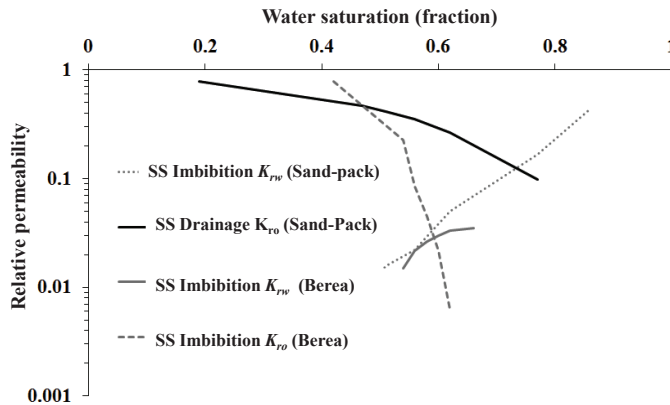


Fig. 3. Steady-State Imbibition relative permeabilities vs average water saturation performed.

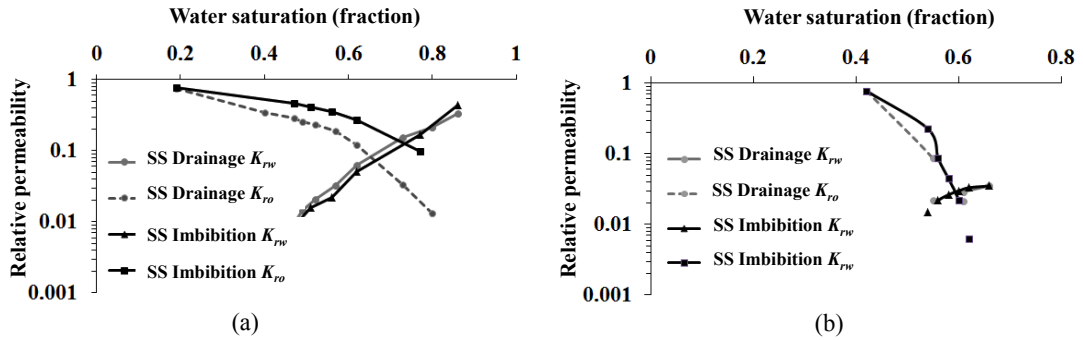


Fig. 4. Steady-State Imbibition and Drainage relative permeabilities performed on the (a) sand-pack and (b) Berea core sample.

#### 4. Interpretation of experimental data with LET and Corey model

Experimental relative permeability curves are here interpreted through two commonly employed effective models. We consider the LET [20] and the Corey [21] models.

##### 4.1. LET model

The LET model is typically expressed as

$$K_{rw} = K_{rw}^o \frac{(S_w^*)^{L_w}}{(S_w^*)^{L_w} + E_w(1 - S_w^*)^{T_w}} \tag{1}$$

$$K_{ro} = K_{ro}^w \frac{(1 - S_w^*)^{L_o}}{(1 - S_w^*)^{L_o} + E_o(S_w^*)^{T_o}} \tag{2}$$

where the normalized water saturation is

$$S_w^* = \frac{S_w - S_{wi}}{1 - S_{wi} - S_{or}} \tag{3}$$

Here,  $S_w^*$ ,  $K_{rw}^o$ , and  $K_{ro}^w$  respectively are the normalized water saturation, end point water and oil relative permeability; L, E and T are empirical tuning parameters. Note that L and T respectively describe the lower and upper parts of the curve; E describes the position of the slope (or the elevation) of the curve.

##### 4.2 Corey model

The Corey model is a simple power law function with only one empirical parameter to estimate. This model is typically expressed in terms of the following set of correlations for the oil -water system

$$K_{rw} = K_{rw}^o (S_w^*)^{N_w} \tag{4}$$

$$K_{ro} = K_{ro}^w (1 - S_w^*)^{N_o} \tag{5}$$

Here,  $S_w^*$ ,  $K_{rw}^0$  and  $K_{ro}^w$  are the normalized water saturation, end point water and oil relative permeability, respectively;  $N_w$  and  $N_o$  are parameters to be estimated through model calibration. These parameters drive the curvature of the relative permeability curves.

Figure 4 depicts both Corey and LET models are fitted by a best fit procedure to steady-state imbibition experimental data. For both samples the LET model exhibits sufficient flexibility to adequately reconcile the entire set of experimental data and also it maintains a smooth behavior. The water relative permeability is almost equal for both correlations while s-behaviour of oil relative permeability at low water saturation is very well modeled with LET model. Corey model is described with only two parameters and thus suffer by bias error [22]. This model is not flexible to reconcile the experimental observations in the entire saturation range.

The Akaike Information Criterion (AIC) [23, 24] is employed to discriminate between the two models considered. In this context, the model associated with the smallest value of AIC should be preferred. Table 3 lists the values of AIC obtained. These results highlight that, even as the number of parameters associated with the LET model is considerably higher than what is required for the Corey model, the complexity of the problem justifies favoring the former over the latter.

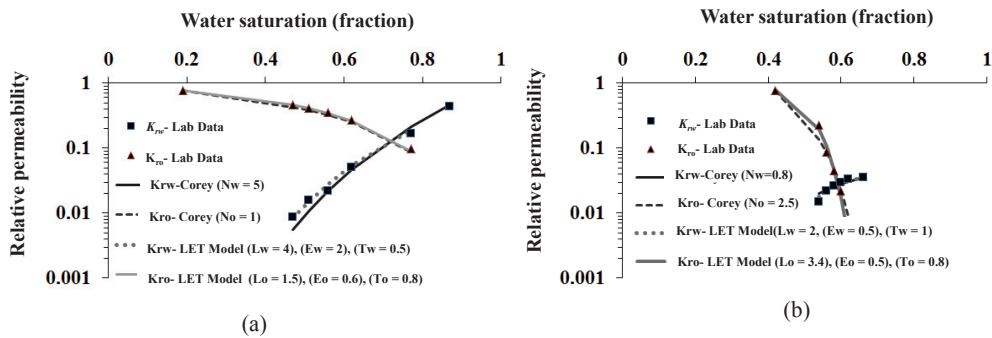


Fig. 5. Steady State Oil-water Relative Permeability vs Water Saturation on (a) sand-pack and (b) Berea: (Laboratory data and interpretation based on the Corey and LET Models)

Table 3. Model identification criteria.

| Samples   | Model identification<br>Criterion | Corey Model |          | LET Model |          |
|-----------|-----------------------------------|-------------|----------|-----------|----------|
|           |                                   | $K_{rw}$    | $K_{ro}$ | $K_{rw}$  | $K_{ro}$ |
| Sand-pack | AIC                               | -56.8       | -52.8    | -59.7     | -56.2    |
| Berea     | AIC                               | -83.3       | -33.1    | -84.6     | -37.4    |

### 5. Conclusions

In this study we performed steady-state two-phase flow characterization experiments through the use of advanced X-ray scanning and appropriate X-ray power settings, chemicals tagging the fluid phases, filters, and collimator configurations. Laboratory measurements of oil-water system relative permeabilities are conducted on the high (sand-pack) and low permeable (Berea sandstone) samples. We

demonstrated the use of X-ray saturation monitoring to provide precise measurements of fluid saturation. The calculated accuracy of saturation determination is almost  $\pm 2\%$ .

Relative permeability estimates are performed with two commonly used interpretive models, i.e., the LET and the Corey model. Application of formal model discrimination criteria based on the AIC metric highlight that, even as the number of parameters associated with the LET model is higher than what is required for the Corey model, the complexity of the problem justifies favoring the former over the latter.

The result obtained from steady-state imbibition and drainage for both samples exhibit some hysteresis effect for oil relative permeability while it has only minute effects for the water relative permeability. This small hysteresis effect for water relative permeability confirms dependency of water relative permeability on its saturation.

## References

- [1] A. Feigl, Treatment of relative permeabilities for application in hydrocarbon reservoir simulation model. *Nafta*. 62(7-8): p. 233-243. 2011
- [2] H. Sharifi Galiuk, H. Alok Bakhtiari, R. Behin, M.R. Esfahani, X-Ray in-situ saturation monitoring, an aid to study relative permeability in water-wet carbonate rocks. *Geopersia*. 2(1): p. 55-66. 2012
- [3] J. Toth, T. Bodi, P. Szucs, F. Civan, Convenient formulae for determination of relative permeability from unsteady-state fluid displacements in core plugs. *Journal of Petroleum Science and Engineering*. 36(1-2): p. 33-44. 2002
- [4] A. Firoozabadi, K. Aziz, Relative Permeabilities From Centrifuge Data. 1991
- [5] C.W. Botermans, D.W. van Batenburg, J. Bruining, Relative Permeability Modifiers: Myth or Reality?, in, *Society of Petroleum Engineers*, 2001.
- [6] R. Liu, H. Liu, X. Li, J. Wang, C. Pang, Calculation of Oil and Water Relative Permeability for Extra Low Permeability Reservoir, in, *Society of Petroleum Engineers*, 2010.
- [7] M.M. Kikuchi, C.C. Branco, E.J. Bonet, R.M. Zanoni, C.M. Paiva, Water Oil Relative Permeability Comparative Study: Steady Versus UnSteady State. 2005
- [8] J. Osoba, J. Richardson, J. Kerver, J. Hafford, P. Blair, Laboratory measurements of relative permeability. *Journal of Petroleum Technology*. 3(02): p. 47-56. 1951
- [9] J. Richardson, J. Kerver, J. Hafford, J. Osoba, Laboratory determination of relative permeability. *Journal of Petroleum Technology*. 4(08): p. 187-196. 1952
- [10] E. Johnson, D. Bossler, V. Bossler, Calculation of relative permeability from displacement experiments. 1959
- [11] S.C. Jones, W.O. Roszelle, Graphical Techniques for Determining Relative Permeability From Displacement Experiments. 1975
- [12] M. Honarpour, S. Mahmood, Relative-permeability measurements: An overview. *Journal of Petroleum Technology*. 40(08): p. 963-966. 1988
- [13] M. Honarpour, L. Koederitz, A.H. Harvey, Relative permeability of petroleum reservoirs, C.R.C. Press, 1986.
- [14] A. Chen, A. Wood, Rate effects on water-oil relative permeability, in: *Proceedings of the International Symposium of the Society of Core Analysts*, Edinburgh, Scotland, 2001, pp. 17-19.
- [15] F. Torabi, O. Zarivnyy, N. Mosavat, Developing New Corey-Based Water/Oil Relative Permeability Correlations for Heavy Oil Systems, in, *Society of Petroleum Engineers*, 2013.
- [16] D.G. Avraam, A.C. Payatakes, Flow regimes and relative permeabilities during steady-state two-phase flow in porous media. *Journal of Fluid Mechanics*. 293: p. 207-236. 1995
- [17] D. Maloney, X-ray imaging technique simplifies and improves reservoir-condition unsteady-state relative permeability measurements. *Petrophysics*. 44(4): p. 271-278. 2003
- [18] A. Laird, J. Putnam, Fluid saturation in porous media by X-ray technique. *Journal of Petroleum Technology*. 3(10): p. 275-284. 1951
- [19] R. Behin, H. Sharifi Galiuk., Study of Two Phase Fluid Flow in Water Wet Reservoir Rocks by Using X-Ray In situ Saturation Monitoring. *Journal of Petroleum Science and Technology*. 1(1): p. 15-23. 2011
- [20] F. Lomeland, E. Ebeltoft, W.H. Thomas, A new versatile relative permeability correlation, in: *International Symposium of the Society of Core Analysts*, Toronto, Canada, 2005, pp. 21-25.
- [21] A.T. Corey, The interrelation between gas and oil relative permeabilities. *Prod. Monthly* 1954
- [22] P. Kerig, A. Watson, Relative-permeability estimation from displacement experiments: an error analysis. *SPE Reservoir Engineering*. 1(02): p. 175-182. 1986



- [23] H. Bozdogan, Model selection and Akaike's Information Criterion (AIC): The general theory and its analytical extensions. *Psychometrika*. 52(3): p. 345-370. 1987
- [24] C.M. HURVICH, C.-L. TSAI, Regression and time series model selection in small samples. *Biometrika*. 76(2): p. 297-307. 1989